Consistency of Geosat, SSM/I, and *ERS-1* Global Surface Wind Speeds—Comparison with In Situ Data

J. BOUTIN AND J. ETCHETO

Laboratoire d'Océanographie Dynamique et de Climatologie, UMR121:CNRS/ORSTOM/Université Pierre et Marie Curie, Paris, France

(Manuscript received 27 December 1994, in final form 6 July 1995)

ABSTRACT

The authors compare wind speed retrieved from the Geosat altimeter, from two Special Sensor Microwave/Imager (SSM/I) microwave radiometers, the SSM/I F08 and SSM/I F10, and from the European Space Agency *ERS-1* scatterometer. As ground truth, ship reports were used that provide a continuous time series of consistent measurements at large scale during the whole period covered by the three satellites, and TOGA TAO data in the tropical Pacific Ocean that are more accurate though more limited in geographical extent than ship wind speeds.

It is evidenced that the Geosat wind speed retrieved using the Witter and Chelton algorithm is underestimated at high wind speed. The authors find that the SSM/I wind speeds retrieved by the Wentz algorithm are underestimated by more than 1 m s^{-1} with respect to the ship wind speeds in large regions at high latitudes, this effect being larger with SSM/I F10 than with SSM/I F08. The authors compare the *ERS-1* wind speeds retrieved from the Cersat preliminary algorithm and from the ESA CMOD4 algorithm; while the former gives wind speeds consistent with the ship measurements, the latter is shown to overestimate low wind speed and to highly underestimate high wind speed. A comparison of the *ERS-1* and SSM/I F10 gridded data shows a 0.5–1 m s^{-1} overestimate of the SSM/I wind speed in the western tropical Pacific and in the intertropical convergence zone and south tropical convergence zone strengthening that the SSM/I wind speeds are disturbed in regions of high atmospheric water content.

1. Introduction

Satellite remotely sensed measurements are of great interest in oceanographic and atmospheric sciences as they provide a global survey of environmental parameters both in space and time, precious information for climatological monitoring. Among the parameters retrieved from remotely sensed data, the scalar wind speed near the sea surface is of particular interest as it is involved in air–sea fluxes determination, such as heat fluxes (Esbensen et al. 1993; Liu 1988) and CO_2 fluxes (Etcheto and Merlivat 1988).

The scatterometer is the most appropriate sensor for measuring the wind velocity with a global coverage: its swath is several hundreds kilometers wide; it is less polluted by land areas than a passive microwave radiometer and unaffected by water vapor, cloud liquid water, and rain of light intensity (Cardone et al. 1983). Unfortunately, no scatterometer providing measurements for periods long enough to allow for a long-term monitoring flew before 1991: Seasat flew only during three months in 1978, and *ERS-1* has been operational since its launch in July 1991. Alternatively, wind modulus measurements have been provided by other satellite-borne sensors: altimeters (Carter et al. 1992; Witter and Chelton 1991) as well as microwave radiometers (Abbott and Chelton 1991; Wentz 1992) make long time series available.

Before using such datasets for climate monitoring, it is essential to check that they are consistent both on small and large scale and to assess the accuracy of the measurements taking into account the scale at which they are used. Usually, the validation is made only in limited areas where buoy measurements exist, thus avoiding worldwide situations: very low or high wind speeds and extreme sea states. This can lead to the nondetection of inversion algorithm or instrument flaws (Boutin and Etcheto 1990; Francis 1987).

In this paper, we compare satellite wind speeds retrieved from the Geosat altimeter, from the F08 and F10 Special Sensor Microwave/Imager (SSM/I) and from the *ERS-1* scatterometer with voluntary ship wind speeds reports. Although they are of poor quality (Pierson 1990), they provide a continuous time series of consistent wind speed measurements at large scale during the whole period covered by the three satellites, as opposed to wind fields deduced from meteorological models, like the European Centre for Medium-Range Weather Forecasts (ECMWF), which have large discontinuities due to model changes (Halpern et al.

Corresponding author address: Dr. J. Boutin, Lab. d'Océanographie Dynamique et de Climatologie, UPMC-Tour 14-2è étage boite 100, 4, Place Jussieu, 75252 Paris, Cedex 05, France.
E-mail: jb@lodyc.jussieu.fr

1994). We also compare the satellite wind speeds with one another when they have simultaneous operating periods, that is, Geosat with SSM/I F08 in 1988, SSM/I F08 and SSM/I F10 in November 1991, and SSM/I F10 and *ERS-1* in 1992. To look at the measurements quality, we collocate the full-resolution wind speeds. To spatially locate the discrepancies, we compare space and time averages. To clarify the Geosat–SSM/I F08 differences in the tropical Pacific Ocean, we also compare the Geosat and SSM/I data with the in situ Tropical Ocean Global Atmosphere (TOGA) Tropical Atmosphere Ocean (TAO) array wind measurements (McPhaden 1993).

2. Data

a. Geosat data

The U.S. Navy's Geosat satellite was launched on 12 March 1985 into a 800-km altitude, 108° inclination orbit. We use the measurements made during the Exact Repeat Mission in 1988 when the satellite was into a 17-day exact repeat orbit.

We use the radar backscatter cross-section measurements (σ_0) provided by the National Oceanic and Atmospheric Administration on the Geophysical Data Records (GDR) tapes.

The spatial resolution of σ_0 is about 10 km, depending on the sea state. We sort the measurements as follows: only the data with 6 dB $\leq \sigma_0 \leq$ 18 dB, $\sigma_h \leq 10$ cm, and 0° < pointing angles $\leq$ 1.1° are kept, where σ_h is the standard deviation of the sea surface height computed when the 10 per second measurements are averaged to produce the 1-s^{-1} data written on the GDR tape. This sorting is fully described in Etcheto and Banege (1992). The first two tests eliminate most of the measurements polluted by ice, land, and rain; the last one eliminates measurements of doubtful accuracy.

We convert σ_0 into wind speed at 10-m height using the Witter and Chelton (1991) algorithm that has recently been supported by several validation studies (Carter et al. 1992; Freilich and Dunbar 1993). A comparison between the Geosat wind speeds retrieved using this algorithm and buoy measurements showed a root-mean-square (rms) difference of 1.9 m s^{-1} (Witter and Chelton 1991).

b. SSM/I data

We use data from the first and second SSM/I that were launched on 19 June 1987 and 1 December 1990 on the U.S. Air Force Defense Meteorological Satellite Program spacecraft F08 and F10, respectively. The orbital parameters of F08 and F10 are not exactly the same: both are near circular and near polar, with an inclination of 98.8°. F08 is sun synchronous, while F10, due to a malfunction during launch, is not exactly sun synchronous: its local equatorial crossing time is increasing at a rate of 47 min per year. Their mean altitudes are 860 and 805 km, and their orbital periods are 102 and 101 minutes for F08 and F10, respectively (Wentz 1991). Consequently, their ground tracks are shifted in space and time, and in November 1991 they were almost out of phase. A complete description of the SSM/I instrument can be found in Hollinger (1989). Its swath is 1400 km wide. At latitudes larger than 40° and at the equator, the coverage is nearly complete after one day; over the global ocean, it is nearly complete after 4 days (Minster et al. 1992).

We use the wind speed derived by Wentz (1992). The retrieval algorithm is based on a geophysical model, and as it is physically based, one can expect that it gives better results on a worldwide scale than algorithms based on regressions between SSM/I brightness temperatures and buoy measurements such as the D-matrix algorithm developed by Goodberlet et al. (1989). A comparison between the retrieved SSM/I wind speed and buoy measurements shows an rms difference of 1.6 m s^{-1} (Wentz 1992), while the D-matrix algorithm gives rms differences greater than 2 m s^{-1}. In addition, the Wentz algorithm is the only one routinely applied to all the SSM/I measurements since July 1987, thus allowing long-term studies. Recently, Busalacchi et al. (1993) compared SSM/I wind stresses deduced from the Wentz's SSM/I wind speeds, with several meteorological model analyses in the tropical Pacific Ocean from July 1987 to June 1988 that showed very encouraging results, as the differences between the SSM/I and the models are on the same order of magnitude as the differences between the different models they used. However, systematic overestimates of the wind in regions of high atmospheric water content like the equatorial Pacific have been evidenced (Halpern 1993; Waliser and Gautier 1993), as well as systematic biases due to an effect of the wind direction in the case of moderate to high wind regimes that are not taken into account in the algorithm routinely applied (Esbensen et al. 1993; Wentz 1992). This can lead to 1 to 2 m s^{-1} regional biases. Halpern et al. (1994) also found that the SSM/I wind speeds are underestimated with respect to the ECMWF wind speeds in the high latitudes of the Northern Hemisphere. As the latter are consistent with the Comprehensive Ocean–Atmosphere Data Set (COADS) wind speeds that are deduced from ship reports, they attribute this difference to the use of ship wind measurements in the ECMWF assimilation that may be stronger at high wind speed than the buoy wind measurements used to calibrate satellite data.

The wind speed, originally retrieved at 19.5-m height, $U_{19.5}$, is converted into a 10-m height wind speed, U, using a neutral atmospheric profile and a drag coefficient equal to 1.5×10^{-3}: $U = 0.939U_{19.5}$. The resolution of the retrieved wind speed is 25 km. Following the Wentz recommendations (Wentz 1989), we discard $U_{19.5}$ less than -4 m s^{-1} and we consider the $U_{19.5}$ values between 0 and -4 m s^{-1} to be 0 m s^{-1}.

We also discard U when the liquid water content is greater than 25 mg cm^{-2}. To avoid any pollution by land area and as this study is not focused on coastal measurements, we add a mask around land areas, 111 km away from large landmasses and 56 km away from islands (diameter less than 150 km) using the method described in Ozieblo and Etcheto (1991). For SSM/I F08, we use only the "class 0" measurements defined in Wentz (1989) and corresponding to water surface measurements far from ice or land and rain rate less than 1.5 mm h^{-1}. For SSM/I F10, we use the class 0 and class 1 measurements newly defined in Wentz (1993): class 0 corresponds to measurements far from land, and class 1 to measurements in a possible ice zone. We keep the class 1 measurements because we observe that the ice sorting of newly defined class 0 is too severe: the southern ice boundary is about 5° north of the one defined by the class 0 of SSM/I F08. Then, we keep class 1 measurements and we add a mask 168 km away from class 6 measurements that detect sea ice as was suggested by F. Wentz (1993, personal communication) and following the method described in Ozieblo and Etcheto (1991).

c. ERS-1 *data*

The European Space Agency *ERS-1* satellite was launched in July 1991, into a 785-km altitude, 98.5° inclination orbit. We use the AMI scatterometer wind speeds retrieved from the radar cross-sectional measurements (σ_0) by two different algorithms: the preliminary algorithm developed by the Centre ERS d'Archivage et de Traitement (CERSAT) for the off-line data processing (Quilfen 1993) and the CMOD4 algorithm (Offiler 1994) used by the European Space Agency for the real-time data processing. (The wind speed is referenced to 10-m height above the sea level.) A comparison of the CERSAT-retrieved wind speeds with mooring measurements shows a 1.2 m s^{-1} rms difference (Quilfen 1993; Quilfen and Bentamy 1994). We take the dealiased wind speed above 3 m s^{-1} and the rank 1 solution for wind speeds below 3 m s^{-1} that are not dealiased. A comparison of the CMOD4-retrieved wind speeds with in situ data off the coast of Norway shows a 1.9 m s^{-1} rms difference when all the measurements are considered and a 1.5 m s^{-1} rms difference when only the best quality measurements are kept, the high wind speeds being excluded (Offiler 1994).

The scatterometer swath is 500 km wide. Each σ_0 has a 50-km resolution and is interpolated on a 25-km square grid, so that adjacent σ_0 are not independent and the resolution of the retrieved wind speed is between 40 and 50 km.

d. *Ship data*

For large-scale validation, we use the wind speeds measured by the voluntary observing ship (VOS) and provided by Météo-France during 1988, 1992, and 1993 over the global ocean. We consider that the measurements are made at 19.5-m height above the sea level as it is close to the mean height of the ship anemometers for measured winds. For visually estimated high winds referenced at 10 m, Kent et al. (1993) found an overestimate that is close to the conversion factor between 10 and 19.5 m, assuming a neutral atmosphere profile. We convert them into 10-m height wind speeds using the same conversion factor as for the SSM/I. We exclude the redundant records and the wind speeds greater than 30 m s^{-1} because they are likely to correspond to erroneous measurements and because the satellite is not sensitive in such a high wind speed range. We also discard ship measurements located less than 100 km away from land as microwave measurements are likely to be disturbed by fetch effects (Glazman 1991). Before doing the collocations, in order to reduce the computation time, we average the ship data closer in space at ±0.125° in latitude and longitude and ±0.5 h in time. We check that this does not modify the statistics of the comparisons, because this applies to only 30% of the data, and the average involves in most of the cases only two measurements.

The main advantage of the ship data is that they are widely spread over the World Ocean and therefore they provide in situ measurements to validate satellite wind speed in many different meteorological situations. The drawback is that they are of poorer quality than mooring measurements (Pierson 1990): a comparison between VOS and buoys wind speeds shows a 2.7 m s^{-1} rms difference (Wilkerson and Earle 1990).

e. *TOGA TAO data*

To clarify the Geosat–SSM/I F08 differences in the tropical Pacific Ocean, we use Autonomous Temperature Line Acquisition System (ATLAS) mooring and current meter mooring wind speed measurements made within the scope of the TOGA TAO program in October and December 1988. They are located in the Pacific Ocean at 110°W (2°S, 0°, 2°N, 5°N), at 124°W (0°), at 140°W (2°S, 0°, 2°N, 5°N, 7°N, 9°N), at 170°W (0°), and at 165°E (5°S, 2°S, 0°N, 5°N). The wind speeds are measured at 4-m height above the sea level with a wind recorder mounted on a surface toroid. The calibration accuracy of the TAO wind sensors is 0.2 m s^{-1} (Mangum et al. 1994). We convert the 4-m height wind speed U_4 into a 10-m height wind speed U using a neutral atmospheric profile and a drag coefficient equal to 1.5×10^{-3}: $U = 1.097U_4$. Details concerning the instrument characteristics can be found in Hayes et al. (1991) and a description of the TOGA TAO array is given in McPhaden (1993).

The TAO wind speeds are hourly, 2- and 6-h averages of the north–south and east–west wind components, depending on the mooring. To keep the same temporal resolution for all the moorings, we take the

6-h average of the 1- and the 2-h resolution wind speeds and we use 6-h averages in our comparisons. Taking the wind components average instead of the wind modulus one can lead to a systematic underestimate of the average of the wind modulus (Etcheto and Merlivat 1988). For instance, Mangum et al. (1992) found that the rms difference between the daily modulus average and the daily components average of the ATLAS wind speed is equal to 0.72 m s^{-1} at 165°E where the effect is maximum because the wind direction is the most variable and to 0.24 m s^{-1} at 110° and 140°W.

3. Methods of comparison

a. *Collocations*

The data periods and the space and time radius used for the collocations are reported in Table 1. For the satellite–ship comparisons, as the ship measurements are mainly located in the Northern Hemisphere, we choose periods of comparison distributed among the four seasons to obtain several wind regimes. For the satellite–satellite comparisons, the measurements are located over the whole ocean covering several wind regimes, and therefore, to reduce the computation time, we use only a 6-day period. For the ship–satellite collocations, the space radius is chosen to match approximately the resolution of the satellite data; the 1-h time radius is equivalent to a space radius of about 25 km for a 7 m s^{-1} wind speed, assuming an equivalence between time and space scales. The choice of a space and time radius for the satellite–ship collocation results from a compromise between the scattering due to the natural space and time variability and the one due to the statistical error: the smallest is the radius, the smallest is the number of points, and the highest is the statistical error, while the effect of the natural variability is minimized. As a test, we double the time radius used for the satellite–ship collocations (±2 h; results not shown). In all the cases, the number of points is doubled but the scattering is not improved, the natural variability compensating for the improvement of the statistical error. For the satellite–satellite collocations, as both SSM/I are out of phase, only the latitudes north of 40°N and south of 40°S are sampled when a 1-h collocation radius is taken. Therefore, we use a 2-h collocation radius for all the satellite–satellite collocations to sample all the latitudes. The space radius is chosen to match approximately the largest resolution of the satellites.

We define the reference measurement as the measurement that governs the extraction of the satellite measurements located at plus or minus the time and space radius; it is either ship data in the ship–satellite collocations or satellite data having the worst spatial resolution in the satellite–satellite collocations. We average all the extracted wind speeds corresponding to one reference wind speed and obtain a pair of collocated measurements, having approximately the same resolution in the case of the satellite–satellite collocations. We discard likely erroneous pairs for which the wind difference is greater than $\langle \Delta U \rangle \pm 3\sigma$, where $\langle \Delta U \rangle$ is the average of the wind difference and σ is the standard deviation of the wind difference computed in 2 m s^{-1} classes. In all cases, this concerns less than 2% of the pairs.

b. *Comparisons of grids*

To spatially locate the satellite–satellite differences, we compare 2.5° × 2.5° resolution grids. The comparisons are made during 1 year for Geosat–SSM/I F08 (25 January 1988–3 February 1989) and during 9.5 months for *ERS-1*–SSM/I F10 (16 March 1992–31 December 1992), which is the longest overlapping period available.

The comparisons are made using data gridded at 2.5° × 2.5° and 2-week resolution for SSM/I and *ERS-1*

TABLE 1. Space and time radius used in the collocations.

Collocation type	Satellite resolution (km)	Period of collocation	Space radius	Time radius (h)
Geosat–ship	10	January–December 1987	0.05° lat 0.50° long	1
SSM/I F08–ship	25	2 weeks per month in February, June, August, and December 1988	0.15° lat 0.15° long	1
SSM/I f10–ship	25	2 weeks per month in February, June, August, and December 1992	0.15° lat 0.15° long	1
ERS-1–ship	~40	August and December 1992 February and June 1993	0.25° lat 0.25° long	1
Geosat–SSM/I F08	10–25	25–31 January 1988	0.125° lat 0.125° long	2
SSM/I F08–SSM/I F10	25–25	1–5 November 1992 (1 point out of 30)	0.125° lat 0.125° long	2
SSM/I F10–*ERS-1*	25–~40	1–5 December 1992 (1 point out of 25)	0.25° lat 0.25° long	2

and 17-day resolution for Geosat. The 2-week resolution has been chosen to be consistent with the Geosat cycle duration (17 days) and is defined to be half of the month. The two SSM/I "weeks" are chosen to match the Geosat cycles as well as possible: on average for each of the 22 studied cycles the length of time nonsimultaneously covered is 3.4 days. For Geosat, we keep the raster only if it contains more than 40 measurements per 17 days; for SSM/I and *ERS-1* the minimum number of measurements per raster and per "week" is 50 and 15, respectively. These thresholds are those we routinely apply to the data; they are chosen to give both a good global coverage of the ocean and reasonable statistics in one raster.

We determine the differences of the 2.5° × 2.5° grids for each 2-week period and we average the 2.5° rasters in 10° rasters: the latter reduces the scatter due to the bad Geosat sampling. We get 22 and 16 grids for the (Geosat–SSM/I) and (*ERS-1*–SSM/I) differences, respectively, at 10° and 2-week resolution, showing the difference between the instruments. We then compute the average and the standard deviation of the grids (22 and 16), obtaining an average grid and a standard deviation grid at 10° resolution. We do not keep the 10° squares for which more than two periods of 2-week duration have no measurement.

We do not present a similar study for the ship–satellite wind speeds, because there is little ship measurements in a 2.5° square and consequently large differences are expected to come from the absence of ship–satellite collocation, nor for the SSM/I F08–SSM/I F10 wind speeds, because we get only one month of overlapping data with several data holes that introduce large scatter due to the different time and space sampling.

4. Results

a. Ship–satellite collocations

Although the ship data are the in situ data covering the largest ocean area, they are preferentially located along sea routes in the Northern Hemisphere, as shown in Fig. 2 of Etcheto and Banege (1992). Consequently, the following results are mainly applicable to the northern latitudes.

We compute the average and the rms of the difference between the ship and the satellite wind speed per 1 m s^{-1} ship wind speed intervals (Fig. 1). Part of the negative differences at low wind speed and positive differences at high wind speed are due to the different resolution of the ship and satellite measurements and to the ship data noise. We estimate these effects by comparing punctual ship measurements with their average made over a square that simulates the satellite integration space, that is, 0.1° × 0.1° and half an hour for the Geosat simulation, 0.3° × 0.3° and 1 h for the SSM/I simulation, and 0.4° × 0.4° and 1 h for the *ERS-1* simulation. We use 12 months of ship data (January–December 1992) and we keep the average only if it includes at least four measurements. This average both simulates the satellite space integration and reduces the ship data noise by at least a factor of 2 as it includes at least four measurements. Figure 2 shows the difference and the rms of the difference between punctual and averaged ship wind speeds for the three simulations. The statistics of the comparisons are reported in Table 2: $\langle U_{\text{ship}} - \langle U_{\text{ship}} \rangle \rangle$ is the mean difference, $\sigma_{\Delta U}$ is the rms of the difference, $\langle U_{\text{ship}} \rangle$ is the average of the ship wind speed, and N is the number of pairs. As expected, the smaller the integration square, the smaller the rms difference. Between 3 and 15 m s^{-1}, the rms of the Geosat simulation is half the one of the SSM/I simulation and 0.4 times the one of the *ERS-1* simulation. These rms's result from both time and space variability of the wind speed and are consistent with the study of Monaldo (1988), who finds a 1 m s^{-1} rms difference between buoy wind speed estimates made one hour apart (time variability) and a 0.6 (0.7) m s^{-1} rms difference between two Geosat wind speed estimates made 30 (40) km apart (space variability). Between 3 and 15 m s^{-1}, the differences are negligible whatever the simulation. Above 15 m s^{-1}, the differences increase: up to 20 m s^{-1}, the differences are still less than 1 m s^{-1} for both Geosat and SSM/I simulations, whereas they reach 1.3 m s^{-1} for *ERS-1*. Above 20 m s^{-1}, the differences are highly increased: the mean differences are 3.5 and 4.6 m s^{-1} for the SSM/I and *ERS-1* simulations, respectively. Unfortunately, due to the small integration space, we do not obtain Geosat simulations for wind speed greater than 20 m s^{-1}.

As the differences between punctual and averaged ship wind speed are negligible between 3 and 15 m s^{-1}, we report the statistics of the ship–satellite comparisons in Table 3 for three wind speed ranges: 0–30 m s^{-1}, 3–15 m s^{-1}, and 15–30 m s^{-1}; $\langle U_{\text{ship}} - U_{\text{sat}} \rangle$ is the mean difference, $\sigma_{\Delta U}$ is the rms of the difference, $\langle U_{\text{ship}} \rangle$ is the average of the ship wind speed, and N is the number of pairs.

1) GEOSAT–SHIP

There are on average 1.9 Geosat measurements collocated with one ship measurement. The rms difference reported in Table 3 between 3 and 15 m s^{-1} is 17% higher than the one obtained by Witter and Chelton (1991) in a comparison with buoy data and shows the high scatter of the ship reports. The mean differences in 1 m s^{-1} intervals of ship wind speed (Fig. 1a) are inside the rms difference up to 15 m s^{-1} and they become greater than the rms difference above 15 m s^{-1}. However, above 10 m s^{-1}, they are larger than the expected differences due to the satellite space integration (see Fig. 2a) and they exceed 1 m s^{-1} above 12 m s^{-1}. This can be due either to an overestimate of the ship wind speeds or to a saturation of the altimeter wind

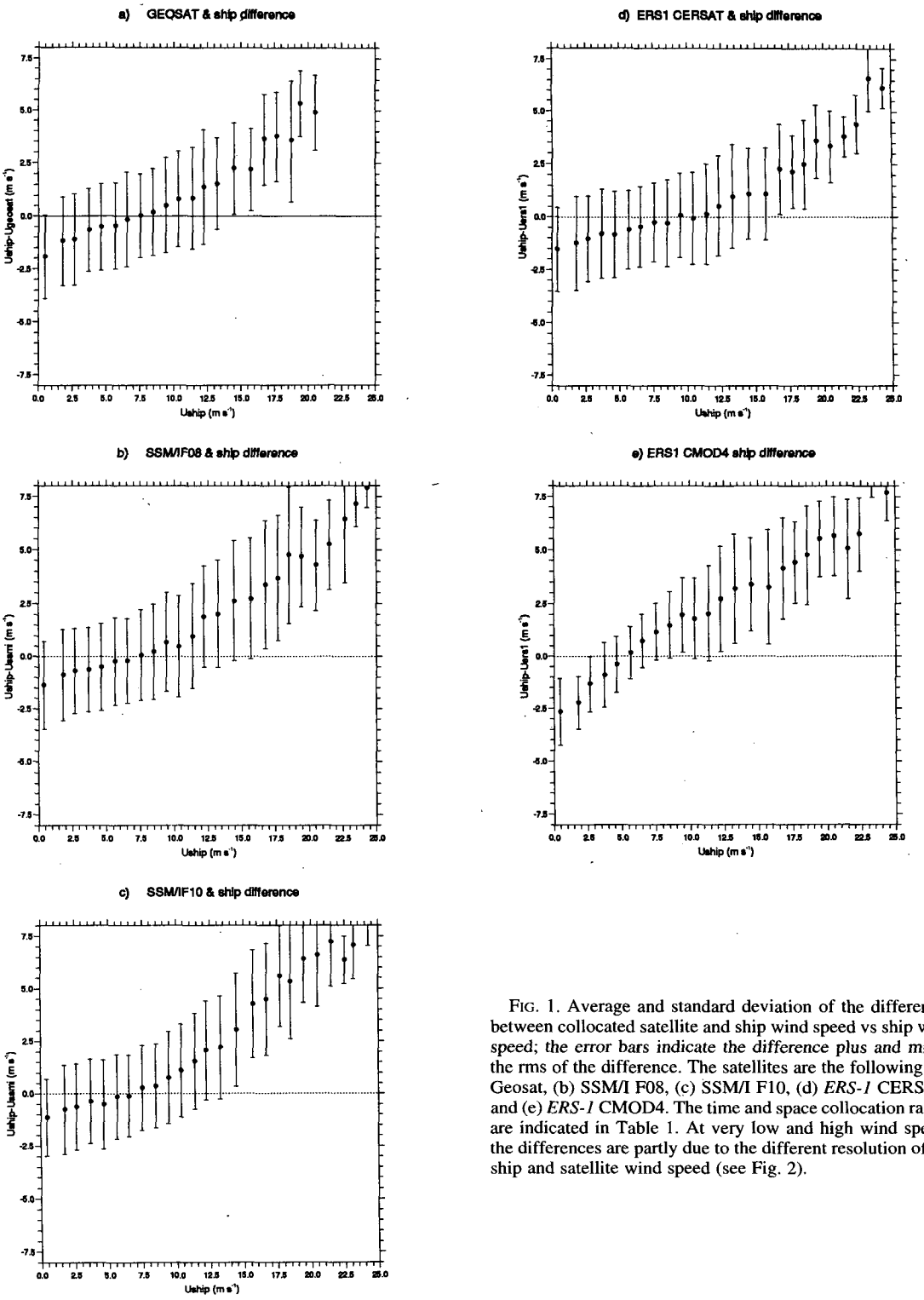

FIG. 1. Average and standard deviation of the differences between collocated satellite and ship wind speed vs ship wind speed; the error bars indicate the difference plus and minus the rms of the difference. The satellites are the following: (a) Geosat, (b) SSM/I F08, (c) SSM/I F10, (d) *ERS-1* CERSAT, and (e) *ERS-1* CMOD4. The time and space collocation radius are indicated in Table 1. At very low and high wind speeds the differences are partly due to the different resolution of the ship and satellite wind speed (see Fig. 2).

speeds. Following previous comparisons of ship wind speeds with in situ or model wind speed (Kent et al. 1993; Wilkerson and Earle 1990) and as we have already lowered the ship wind speeds when making the height correction, a systematic overestimate of more than 2 m s^{-1} of the wind speeds greater than 15 m s^{-1}

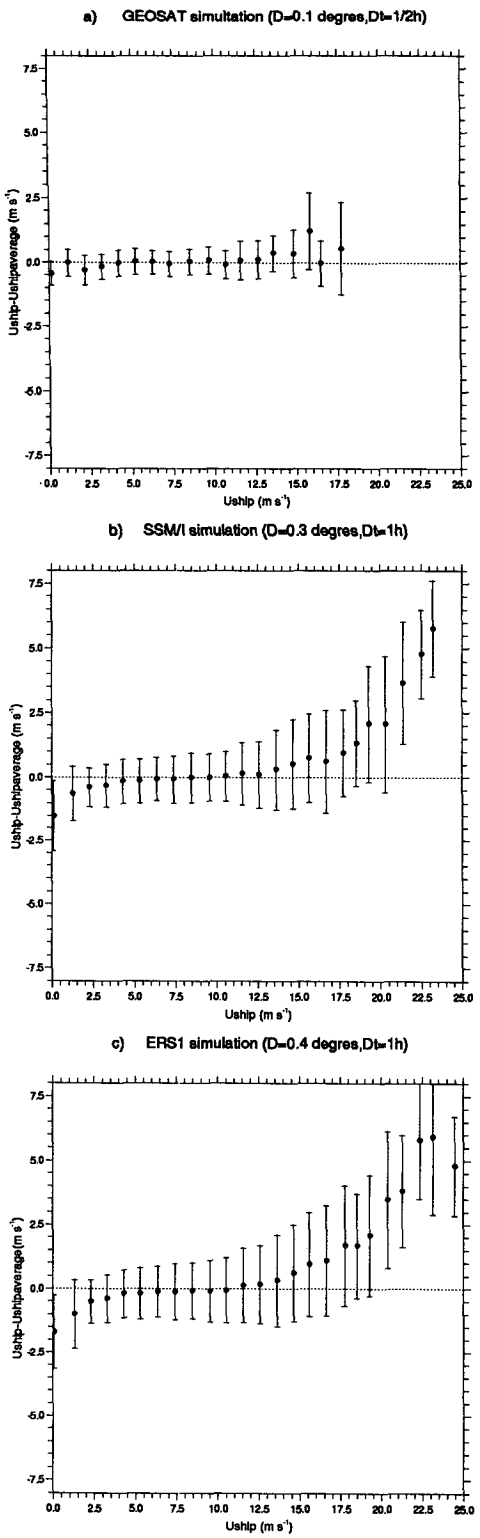

FIG. 2. Average and standard deviation of the differences between averaged and nonaveraged ship wind speed vs nonaveraged ship wind speed. The average is made over three time and space diameters simulating three instruments: (a) 0.5 h and 0.1° (Geosat altimeter); (b) 1 h and 0.3° (SSM/I microwave radiometer); (c) 1 h and 0.4° (*ERS-1* scatterometer).

is unlikely. On the other hand, it is well known that the sensitivity of an altimeter to high wind speeds is reduced, although it is not clear whether the altimeter signal completely saturates or if it is possible to retrieve high wind speed with a modified algorithm calibrated with high wind speeds as was proposed by Young (1993).

2) SSM/I–SHIPS

There are on average 1.5 SSM/I measurements collocated with one ship measurement. Above 9 m s^{-1}, the mean differences in 1 m s^{-1} wind intervals (Figs. 1b,c) are much larger than the expected differences due to the satellite space integration (Fig. 2b). They are also higher for SSM/I F10 (larger than 1 m s^{-1} above 10 m s^{-1}) than for SSM/I F08 (larger than 1 m s^{-1} above 11 m s^{-1}), which leads to a ship-SSM/I F10 wind speed difference of 0.4 m s^{-1} instead of 0.2 m s^{-1} for the ship–SSM/I F08 wind difference between 3 and 15 m s^{-1} (Table 3). The rms of the difference for both SSM/I are similar. The rms of the differences are larger than the ones expected from the integration effect and the Geosat ones (Figs. 2a,b), although the rms difference found by Wentz (1992) was lower than the Geosat one found by Witter and Chelton (1991): the rms of the differences in 1 m s^{-1} classes are 15%–26% greater than the Geosat ones below 3 m s^{-1}; they are comparable between 3 and 9 m s^{-1} and they are 10%–25% greater between 9 and 18 m s^{-1}. Below 3 m s^{-1} this result is not surprising, as an altimeter is more sensitive to low wind speed than a microwave radiometer; the differences can also be a result of atmospheric perturbations, as the SSM/I is very sensitive to atmospheric water content (Halpern 1993). Above 9 m s^{-1}, this can be due to directional effects that are dependent on the geometry of the wind velocity and the satellite radiometer viewing direction: these effects are larger at high wind speeds (Wentz 1992), and on average over the ascending and descending orbits, they can lead to an underestimate at high northern latitudes (Esbensen et al. 1993) where most of the ship measurements are located. The Wentz (1992) comparisons were less influenced because the National Oceanic and Atmospheric Administration moorings that he used are located at lower latitudes than most of the ship measurements; Halpern et al. (1994) also argued that buoy anemometer wind measurements that have been used to calibrate the SSM/I algorithm may be lower than ship wind measurements at high wind speed due to the poor quality of both types of measurements.

3) *ERS-1*–SHIPS

There are on average 3.6 *ERS-1* measurements collocated with one ship measurement. Below 3 m s^{-1}, the negative differences observed in Fig. 1e for the CMOD4 algorithm and in Fig. 1d for the CERSAT one

TABLE 2. Comparison of punctual with averaged ship wind speed measurements.

Time and space integration diameter	U_{ship} range (m s^{-1})	$\langle U_{ship} - \langle U_{ship} \rangle \rangle$ (m s^{-1})	$\sigma_{\Delta U}$ (m s^{-1})	$\langle U_{ship} \rangle$ (m s^{-1})	N
0.5 h; 0.1°	0–30	0.00	0.55	6.52	2348
0.5 h; 0.1°	3–15	0.02	0.53	6.88	2119
0.5 h; 0.1°	15–20	0.86	1.42	16.62	23
1 h; 0.3°	0–30	0.00	1.12	7.91	10 344
1 h; 0.3°	3–15	−0.02	1.00	7.83	9229
1 h; 0.3°	15–20	0.94	1.87	16.84	427
1 h; 0.3°	15–30	1.22	2.17	17.38	480
1 h; 0.4°	0–30	0.00	1.40	8.14	14 072
1 h; 0.4°	3–15	−0.06	1.20	7.99	12 323
1 h; 0.4°	15–20	1.27	2.18	16.72	697
1 h; 0.4°	15–30	1.78	2.58	17.54	825

are both due to the satellite integration effect (Fig. 2c) and to the inaccuracy of both the ship measurements and the scatterometer measurements at low wind speed. In particular, the very low CMOD4 differences below 2 m s^{-1} are due to the absence of CMOD4 wind speed estimates below 1.5 m s^{-1}. The statistics of the comparisons shown in Table 3 and in Figs. 2d and 2e for moderate to high wind speeds are different: the CMOD4 wind speeds are systematically biased low above 7 m s^{-1} by 1–3 m s^{-1} more than the difference expected from the satellite space integration (see Fig. 2c), whereas the CERSAT wind speeds are in good agreement with the ship wind speeds when the satellite integration effect is subtracted. This leads to slightly negative differences between 3 and 15 m s^{-1} for the CERSAT algorithm and to positive differences for the CMOD4 algorithm (Table 3). The smaller rms of the differences observed with the CMOD4 algorithm between 3 and 15 m s^{-1} is due to the smaller range of variation of the CMOD4 wind speeds as the standard deviation of the wind speeds between 3 and 15 m s^{-1} is equal to 2.5 m s^{-1} for CMOD4 and to 3.2 m s^{-1} and 3.0 m s^{-1} for the CERSAT and ship wind speeds, respectively. Above 15 m s^{-1}, the CMOD4 algorithm appears to retrieve wind speeds weaker than the results of the CERSAT algorithm (2 m s^{-1} at 20 m s^{-1}), the difference with the ship measurements being well outside the expected integration effect: at 16 m s^{-1}, the CMOD4–ship wind speed difference remains equal to about 1.5 m s^{-1} once the integration effect has been removed; this is in close agreement with the conclusions of Offiler (1994), who suggests that the CMOD4 wind speeds may be underestimated by 1.5 m s^{-1} above 16 m s^{-1}. Above 20 m s^{-1}, the CMOD4 comparison is not reliable as it was made with very little high wind speed measurements, only one *ERS-1* overpass being collocated with wind speeds greater than 20 m s^{-1}. A slight tendency for the CERSAT algorithm

TABLE 3. Satellite and ship wind speed collocations.

Satellite	U_{ship} range (m s^{-1})	$\langle U_{ship} - U_{sat} \rangle$ (m s^{-1})	$\sigma_{\Delta U}$ (m s^{-1})	$\langle U_{ship} \rangle$ (m s^{-1})	N
Geosat	0–30	0.09	2.41	7.29	3525
Geosat	3–15	0.16	2.25	7.73	2900
Geosat	15–30	3.73	2.44	17.74	129
SSM/I F08	0–30	0.23	2.53	7.27	10 414
SSM/I F08	3–15	0.22	2.37	7.62	8488
SSM/I F08	15–30	4.08	3.01	18.25	453
SSM/I F10	0–30	0.48	2.52	7.45	9997
SSM/I F10	3–15	0.44	2.31	7.75	8383
SSM/I F10	15–30	5.27	2.67	17.88	393
ERS-1 CERSAT	0–30	−0.14	2.27	7.92	6743
ERS-1 CERSAT	3–15	−0.21	2.12	7.95	5610
ERS-1 CERSAT	15–30	2.64	2.39	18.19	407
ERS-1 CMOD4	0–30	1.25	2.31	8.45	4313
ERS-1 CMOD4	3–15	1.25	2.03	8.28	3781
ERS-1 CMOD4	15–30	4.49	2.52	17.90	255

to retrieve wind speeds lower than the ship measurements can be seen between 15 and 20 m s^{-1}, the accuracy of the in situ data being insufficient to reach any conclusion above 20 m s^{-1}.

With respect to the previous comparisons, the CERSAT rms of the differences are 6% lower than the Geosat ones and about 10% lower than the SSM/I ones, and the bias in 1 m s^{-1} ship wind speed interval are lower than the SSM/I ones, indicating that the CERSAT estimates are more consistent with the in situ measurements. This confirms the low rms difference between the CERSAT-retrieved *ERS-1* wind speeds and mooring measurements found by Quilfen and Bentamy (1994).

Given the large bias of the CMOD4 algorithm, we will consider only the CERSAT algorithm in the following comparisons.

b. *Satellite–satellite comparisons*

We recall that the space radius used for the collocations matches approximately the largest resolution of the satellites involved in the collocation; therefore, once the satellite wind speeds having the smallest spatial resolution are collocated with a satellite wind speed having the largest resolution and are averaged, the spatial resolution of the paired measurements is about the same and in the following comparisons, no difference coming from the difference of the satellite footprint size is expected.

The mean of the differences, $U_{sat1} - U_{sat2}$, and the corresponding rms are computed in 1 m s^{-1} intervals of the average of the two satellites wind speed, $(U_{sat1} + U_{sat2})/2$, and are presented in Fig. 3. We make the comparisons over the global ocean and north of 20°N to compare the results with the satellite–ship comparisons that are mainly located in the middle and high northern latitudes. The corresponding statistics are reported in Table 4 (global ocean) and in Table 5 (north of 20°N); $\langle U_{sat1} - U_{sat2} \rangle$ is the mean difference, and $\langle U_{sat} \rangle$ is the average of satellite wind speeds.

1) GEOSAT–SSM/I F08

There are about four Geosat measurements collocated with one SSM/I measurement. Between 0 and 10 m s^{-1}, the comparisons over the global ocean and north of 20°N show a slight underestimate of the SSM/I wind speeds. Between 10 and 15 m s^{-1}, the mean differences in the northern latitudes are close to 0.5 m s^{-1}, while they are about 0 when averaged over the global ocean. Moreover, the rms of the differences is higher north of 20°N (Tables 4 and 5). Above 15 m s^{-1}, the Geosat wind speeds appear to be underestimated by several meters per second in both regions. The differences in the northern latitudes are consistent with the ship–satellite comparisons and are attributed to a directional effect of the SSM/I at moderate and high wind speed [see section 4a(2)] and to a saturation of the Geosat altimeter at high wind speed [see section 4a(1)]. The positive differences at high latitudes are clearly seen on the yearly and 10° resolution map of the differences shown in Fig. 4a and computed as described in section 3a. We recall that the measurements were not collocated before doing the grids, and therefore, part of the differences and of the rms of the differences can come from the different space and time coverage of both instruments, especially because the Geosat altimeter measurements are very undersampled. The regions with large positive differences are characterized by high rms of the differences (Fig. 4b) because the directional effect depends on the direction and the intensity of the wind speed that are variable during the whole year. South of 50°S, the negative differences are due to the ice pack proximity since the SSM/I data close to the ice are removed, whereas most of the Geosat measurements are not disturbed by the ice proximity and are included in the raster average. As the wind speed is generally lighter near the ice pack, the Geosat rasters appear to be lower than the SSM/I ones. In the middle tropical Pacific Ocean (10°S–10°N), the SSM/I wind speeds are about 0.5 m s^{-1} higher than the Geosat ones. Waliser and Gauthier (1993) and Halpern (1993) have already made validation studies of the SSM/I wind speeds in the tropical Pacific Ocean using the TAO moorings measurements from July 1987 to June 1988 and in 1989, respectively; they found a poor accuracy of the SSM/I wind speeds in the western tropical Pacific (165°E) that can be attributed to high atmospheric water content in this region. However, the bias seen in Fig. 4a is almost zero in the western Pacific. A La Niña anomaly occurred in 1988 that was associated with reduced SST and convection in the western Pacific (Arkin 1989); consequently, the overestimate of the SSM/I wind speeds associated to high atmospheric water content should be reduced. Therefore, the origin of the negative anomaly seen in Fig. 4a in the tropical Pacific Ocean is not obvious, and in order to clear it, we compare the Geosat and SSM/I wind speeds with the TAO mooring measurements during October and December 1988 when we observe that the Geosat–SSM/I difference was maximum (see section 4c).

2) SSMI F10–SSM/I F08

There are on average 1.2 SSM/I F10 measurements collocated with one SSM/I F08 measurement. The rms difference found over the global ocean (Table 4) is very close to the 1.6 m s^{-1} found by Wentz (1992) when making comparisons with in situ data. It is slightly increased north of 20°N and above 9 m s^{-1} (Table 5 and Fig. 3d) due to the directional bias: as both SSM/I are out of phase, SSM/I F08 ascending passes are collocated with SSM/I F10 descending passes, and vice versa, so that the direction of the wind speed relative to the satellite viewing direction is not

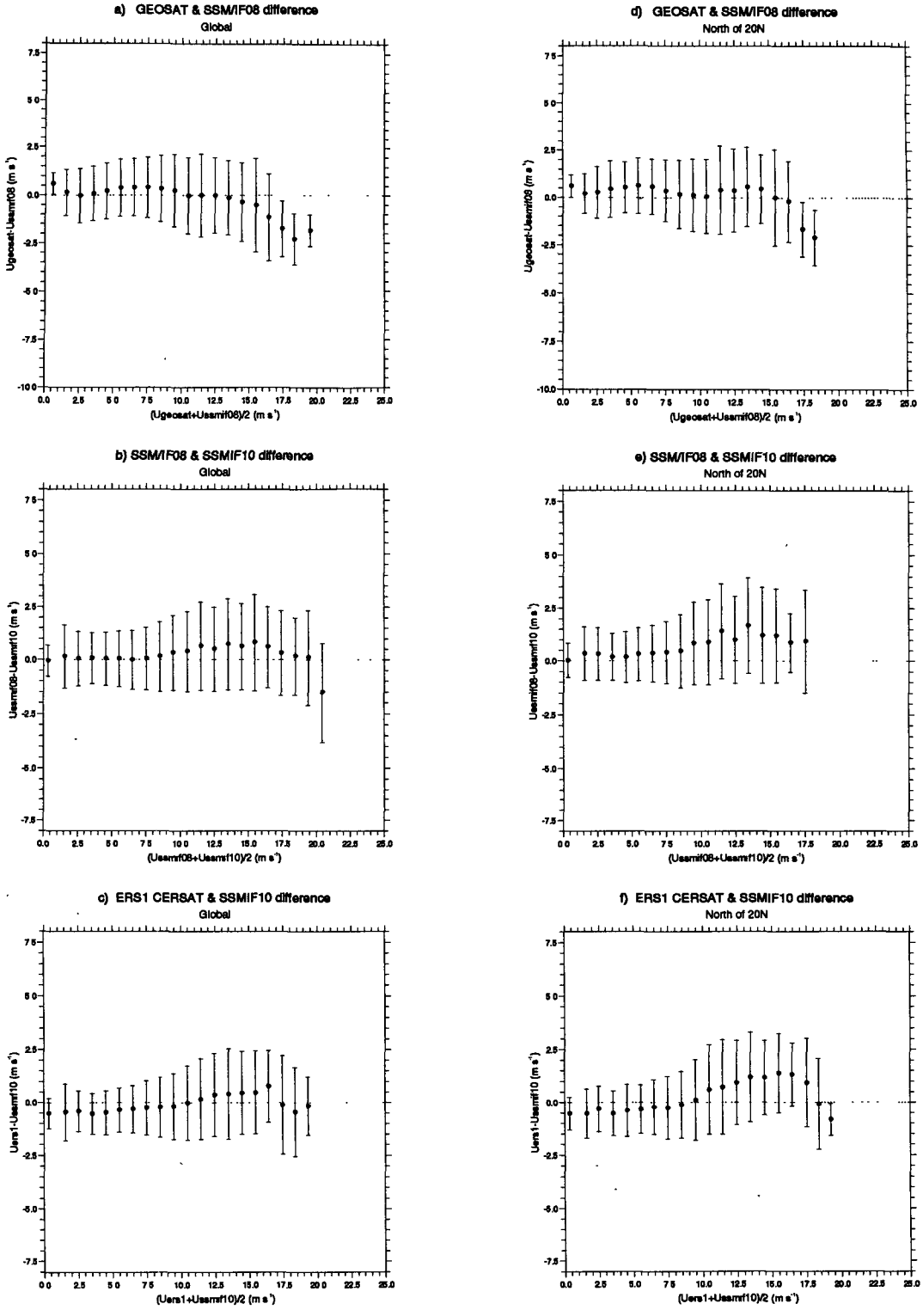

FIG. 3. Difference between collocated satellite wind speeds vs mean satellite wind speed; left, at global scale; right, north of 20°N: (a) and (d) Geosat minus SSM/I F08; (b) and (e) SSM/I F08 minus SSM/I F10; (c) and (f) *ERS-1* CERSAT minus SSM/I F10. The time and space collocation radii are indicated in Table 1.

TABLE 4. Satellite–satellite wind speed collocations over the global ocean.

Satellite 1–satellite 2	$\langle U_{sat} \rangle$ range (m s^{-1})	$\langle U_{sat1} - U_{sat2} \rangle$ (m s^{-1})	$\sigma_{\Delta U}$ (m s^{-1})	$\langle U_{sat} \rangle$ (m s^{-1})	N
Geosat–SSM/I F08	0–30	0.22	1.67	7.34	17 092
Geosat–SSM/I F08	3–15	0.25	1.69	7.76	15 111
Geosat–SSM/I F08	15–30	−1.13	2.16	16.51	318
SSM/I F08–F10	0–30	0.20	1.58	7.63	18 121
SSM/I F08–F10	3–15	0.19	1.58	7.65	16 291
SSM/I F08–F10	15–30	0.58	2.11	16.49	601
ERS-1 CERSAT–SSM/I F10	0–30	−0.18	1.45	7.76	20 492
ERS-1 CERSAT–SSM/I F10	3–15	−0.18	1.45	7.97	18 544
ERS-1 CERSAT–SSM/I F10	15–30	0.39	1.99	16.29	560

$\langle U_{sat} \rangle$ is the average of U_{sat1} and U_{sat2}.

the same for both collocated measurements. Above 9 m s^{-1}, the SSM/I F10 wind speeds are 0.5–1 m s^{-1} lower than the SSM/I F08 ones, and the bias is increased north of 20°N (Figs. 3b and 3d; Tables 4 and 5). This cannot be simply related to a directional effect, for both SSM/Is look alternately over the ocean in the same direction, and therefore, when the collocations are considered over all the descending and ascending passes, the mean difference should be equal to 0. This is consistent with the results of the ship–SSM/I collocations showing that the SSM/I F08 is less underestimated than the SSM/I F10 at high wind speed [see section 4a (2)]. This could be due to the slightly varying incidence angle of SSM/I F10.

3) *ERS-1* CERSAT–SSM/I F10

There are on average 3.7 SSM/I F10 measurements collocated with one *ERS-1* measurement. Below 5 m s^{-1}, the *ERS-1* wind speeds are 0.5 m s^{-1} lower than the SSM/I ones (Fig. 3c) that can probably be explained by a weak sensitivity of the *ERS-1* scatterometer to low wind speeds. The rms of the differences over the global ocean (Table 4) are weaker than in the previous comparisons because in the Geosat comparisons both the SSM/I flaws and the Geosat underestimates at high wind speed were added and in the SSM/I comparisons the directional effects were maxima as both SSM/I are out of phase. As in previous comparisons, the biases are larger north of 20°N than over the global ocean (Figs. 3c and 3f). The positive bias between 10 and 18 m s^{-1} is larger than the one seen in the Geosat–SSM/I comparison and is slightly smaller than the SSM/I F08–SSM/I F10 difference with the same tendency to increase north of 20°N. This is probably due to a combination of the SSM/I F08–SSM/I F10 bias and of the Geosat underestimate at high wind speed. We obtain a similar result with the 10-month comparison of gridded wind speeds (Fig. 4c): at high latitude the bias is larger with *ERS-1* than with Geosat. In the Tropics, negative differences are observed in the western Pacific and along the ITCZ and the STCZ convergence zones, in regions where the atmospheric water content is maximum although the 1992 year is an anomalous one (Chelliah 1994; Mo and Wang 1994). The rms of the gridded differences (Fig. 4d) are about half the ones obtained in the Geosat–SSM/I comparison mainly because of the bad sampling of the Geosat measurements.

c. *Buoy–satellite comparisons*

To clear the Geosat–SSM/I wind speed differences observed in the tropical Pacific Ocean (Fig. 4a), we collocate the Geosat and SSM/I wind speeds with the TAO mooring wind speeds in October and December 1988 when the differences were maxima in the central Pacific. We extract the satellite wind speeds located at ±2° in longitude and ±0.2° in latitude from the TAO mooring and during the 6 h of the TAO averaging period. The statistics of the comparisons computed at five longitudes for TAO wind speeds greater than 4 m s^{-1} are reported in Table 6. Below 4 m s^{-1} the satellite wind speeds are greater than the TAO ones due to their decreased accuracy at low wind speeds.

The rms differences obtained in the SSM/I comparisons are well lower than the ones found by Waliser and Gauthier (1993) who compare daily TAO and SSM/I wind speeds from July 1987 to June 1988. They also compare wind speeds with higher temporal resolution (2-h wind speed) and show that the high temporal resolution has little influence on the result. The high rms differences they found come probably from problems during the 1987 year that were pointed out by Halpern (1993) who compares monthly averages of 1/3° SSM/I wind speeds with TAO monthly wind speeds: he finds rms differences in 1987 to be twice the ones in 1988 and 1989. The latter are about 20% lower than the ones we found, probably because he compares monthly averages. The biases we find at 110° and 140°W are about 0.6 m s^{-1} larger than the ones found by Waliser and Gauthier (1993). This is attributable to

TABLE 5. Satellite–satellite wind speed collocations north of 20°N.

Satellite 1–satellite 2	$\langle U_{sat} \rangle$ range (m s^{-1})	$\langle U_{sat1} - U_{sat2} \rangle$ (m s^{-1})	$\sigma_{\Delta U}$ (m s^{-1})	$\langle U_{sat} \rangle$ (m s^{-1})	N
Geosat–SSM/I F08	0–30	0.32	1.82	8.62	2932
Geosat–SSM/I F08	3–15	0.37	1.82	8.74	2633
Geosat–SSM/I F08	15–30	−0.81	2.23	16.67	118
SSM/I F08–F10	0–30	0.54	1.63	7.26	4087
SSM/I F08–F10	3–15	0.56	1.66	7.67	3676
SSM/I F08–F10	15–30	1.08	2.00	16.09	59
ERS-1 CERSAT–SSM/I F10	0–30	0.19	1.79	9.02	3729
ERS-1 CERSAT–SSM/I F10	3–15	0.15	1.78	8.71	3367
ERS-1 CERSAT–SSM/I F10	15–30	1.07	1.92	16.45	253

$\langle U_{sat} \rangle$ is the average of U_{sat1} and U_{sat2}.

the correction for the height of the measurements that enhance the TAO wind speed by about 10%—that is by about 0.6 m s^{-1}—that they do not make. On the other hand, at 165°E, we find a −0.1 m s^{-1} bias and an rms difference close to the ones at 110° and 140°W, whereas Waliser and Gauthier (1993) found a −1.7 m s^{-1} bias that would be reduced to about −1.1 m s^{-1} after height correction and an rms difference twice the one at 110° and 140°W. Halpern (1993) also finds significantly lower correlation coefficients at 165°E than at 110°W in 1989. This seems to indicate that the SSM/I wind speeds were less polluted by the atmospheric water content at the end of the 1988 year because of the La Niña event, as already suspected in section 4b (1).

The Geosat wind speeds are systematically underestimated with respect to the TAO ones, the minimum of the bias being observed at 165°E. This could be due to an influence of the significant wave height parameter. Carter et al. (1992) have shown that when this parameter is taken into account in the wind speed retrieval model, the accuracy of the wind speed is highly improved. Lefevre et al. (1994), using such a model for the inversion of the Topex–Poseidon data, found higher wind speeds in the Tropics than with the Witter and Chelton (1991) algorithm. We therefore conclude that most of the negative Geosat–SSM/I differences in the Tropics probably come from an underestimate of the Geosat wind speeds.

5. Discussion and conclusions

Although the ship wind speeds were found not to be suitable for calibrating satellite wind speed retrieval algorithms (Pierson 1990) and give larger rms differences than the mooring measurements when making satellite–in situ wind speeds comparisons, they have the great advantage of providing a continuous time series of consistent measurements at large scale over the last 10 years, and we use them as a qualitative reference to analyze the biases between several instruments that did not fly simultaneously. They are punctual and very scattered, which introduces biases in the satellite–ship comparisons. This bias also exists in satellite–mooring comparisons but is smaller since the moorings measurements are less scattered than the ships ones. We quantify these effects by averaging the ship data close in space and time over areas corresponding to the footprint size of the satellite. Moreover, when comparing measurements of two satellites having a different footprint size, we average the highest resolution satellite data to compare data of similar resolution. Once the integration effects are removed from the ship–satellite differences, we evidence satellite versus ship biases that we find also in independent satellite–satellite comparisons made over separate periods. At high wind speed, above about 15 m s^{-1}, the Geosat wind speeds are underestimated with respect to the ship wind speeds and to the SSM/I F08 wind speeds. This effect could be due to a saturation of the altimeter. Above 9 m s^{-1}, both SSM/I wind speeds are 1–2 m s^{-1} weaker than the ship ones, the bias being larger for SSM/I F10. The SSM/I F08 wind speeds are about 0.5 m s^{-1} weaker than the Geosat ones between 10 and 15 m s^{-1}, north of 20°N. The SSM/I F10 wind speeds are lower than the *ERS-1* CERSAT ones between 10 and 18 m s^{-1}, the bias ranging from 0.5 m s^{-1} to 1.5 m s^{-1}. The weaker bias in the Geosat–SSM/I F08 comparison can be explained by both the underestimation of the high Geosat wind speeds and the larger bias of the SSM/I F10. The regional underestimates of the SSM/I wind speeds shown both in the ship–SSM/I comparisons and in the satellite–SSM/I global gridded data comparisons are mostly attributed to directional effects of the SSM/I. The different quality of buoy anemometer wind measurements used to calibrate satellite data and of the ship wind measurements at high wind speed has been put forward by Halpern et al. (1994) to explain underestimates of SSM/I wind speeds with respect to ECMWF wind speeds, but it cannot be the only explanation of the SSM/I underestimates, as the Geosat and *ERS-1* algorithms were also calibrated with buoy anemometer measurements. While the wind speeds re-

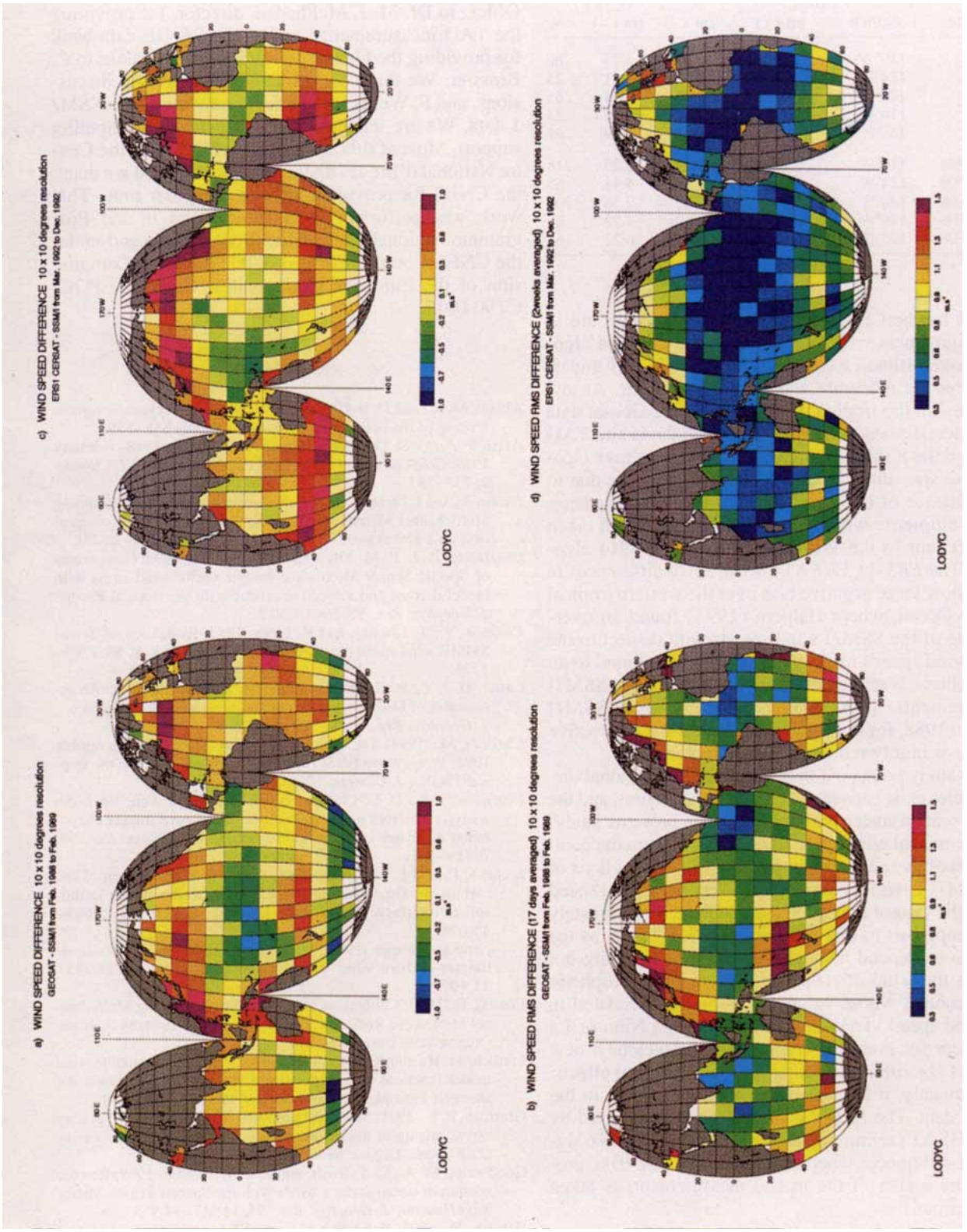

FIG. 4. Maps of the gridded satellite wind speed differences at 10° and 2-week resolution: (a) Geosat minus SSM/I F08; (c) *ERS-1* CERSAT minus SSM/I F10. Maps of the rms of the differences at 10° and 2-week resolution: (b) Geosat minus SSM/I F08; (d) *ERS-1* CERSAT minus SSM/I F10.

TABLE 6. Atlas–satellite wind speed collocations ($U_{atlas} > 4$ m s^{-1}).

Satellite	Longitude	$\langle U_{atlas} - U_{sat} \rangle$ (m s^{-1})	$\sigma_{\Delta U}$ (m s^{-1})	$\langle U_{atlas} \rangle$ (m s^{-1})	N
Geosat	110°W	1.59	1.62	6.77	80
Geosat	124°W	1.51	1.77	6.01	25
Geosat	140°W	0.99	1.56	7.34	65
Geosat	170°W	1.00	1.14	7.45	24
Geosat	165°E	0.58	1.43	6.29	68
SSM/I F08	110°W	1.08	1.09	6.28	218
SSM/I F08	124°W	0.63	1.19	5.48	65
SSM/I F08	140°W	0.22	1.29	7.36	300
SSM/I F08	170°W	−0.06	0.80	7.72	67
SSM/I F08	165°E	−0.12	1.22	6.22	164

trieved by the CERSAT preliminary algorithm are in good agreement with the ship data, the CMOD4 algorithm overestimates the low wind speeds and underestimates the moderate and high wind speeds. At low latitudes, in the tropical Pacific ocean, the Geosat data are underestimated with respect to both the in situ TAO data and the SSM/I F08 data, indicating negative Geosat wind speed bias in this region that could be due to the influence of the significant wave height parameter on the altimetric wind speed retrieval that is not taken into account in the Witter and Chelton (1991) algorithm. The *ERS-1* CERSAT–SSM/I F10 differences in 1992 show large negative bias over the western tropical Pacific Ocean, where Halpern (1993) found an overestimate of the SSM/I wind speeds with respect to the TAO wind speeds in 1989. This bias is attributed to an atmospheric water content disturbance of the SSM/I measurements. It is smaller on the Geosat–SSM/I maps in 1988, for during a La Niña year the convective activity is highly reduced in these regions.

This study points out that very large and regional discrepancies exist between the SSM/I, the Geosat, and the *ERS-1* scatterometer wind speeds. This prevents studying interannual wind speed variability by using the combination of these sensors without previous corrections of the SSM/I flaws and in regions of very high wind speed where the Geosat measurements saturate. Unfortunately this compels us to reprocess all the SSM/I data, as the corrections depend not only on the wind intensity but also on the wind direction as well as the atmospheric water content whose variability is highly correlated to the wind speed variability itself, during El Niño or La Niña year for instance. Wentz (1992) develops a new retrieval algorithm correcting for the directional effects. Unfortunately, it has not been routinely applied to the SSM/I data. The *ERS-1* scatterometer data inverted by the CERSAT preliminary algorithm have not shown significant differences when compared with ship data, provided the scatter of the in situ measurements is taken into account.

Acknowledgments. We are grateful to Ifremer/CERSAT and to Y. Quilfen for providing the *ERS-1* data; to Météo-France for providing the ship reports, with special thanks to T. Ludget; to the TOGA TAO Project Office; to Dr. M. J. McPhaden, director, for providing the TAO measurements; and to the PAVIE data bank for providing the Geosat data, with special thanks to C. Brossier. We thank Dr. McPhaden for fruitful discussions, and F. Wentz for helpful comments on the SSM/I data. We are indebted to A. Ozieblo for computing support. Most of this study was performed on the Centre National d'Etudes Spatiales computer, and we thank the CNES for providing us with computer time. This work was performed with the support of the Programme National de Télédétection Spatiale and under the CNES Contract 90/CNES/0323 and the Commission of the European Communities Contract EPOC-CT90-0017.

REFERENCES

Abbott, M. R., and D. B. Chelton, 1991: Advances in passive remote sensing of the ocean. *Rev. Geophys.*, (Suppl) 555–556.

Arkin, P. A., 1989: The global climate for December 1988–February 1989: Cold episode in the tropical Pacific continues. *J. Climate,* **2,** 737–757.

Boutin, J., and J. Etcheto, 1990: Seasat scatterometer versus Scanning Multichannel Microwave Radiometer wind speeds: A comparison on a global scale. *J. Geophys. Res.*, **95,** 22 275–22 288.

Busalacchi, A. J., R. M. Atlas, and E. C. Hackert, 1993: Comparison of Special Sensor Microwave Imager vector wind stress with model-derived and subjective products for the tropical Pacific. *J. Geophys. Res.*, **98,** 6961–6977.

Cardone, V., T. Chester, and R. Lipes, 1983: Evaluation of Seasat SMMR wind speed measurements. *J. Geophys. Res.*, **88,** 1709–1726.

Carter, D. J. T., P. G. Challenor, and M. A. Srokosz, 1992: An assessment of Geosat wave height and wind speed measurements. *J. Geophys. Res.*, **97,** 11 383–11 392.

Chelliah, M., 1994: The global climate for September–November 1992: Weak warm ENSO episode conditions linger in the tropical Pacific. *J. Climate,* 1565–1580.

Esbensen, S. K., D. B. Chelton, D. Vickers, and J. Sun, 1993: An analysis of errors in Special Sensor Microwave Imager evaporation estimates over the global ocean. *J. Geophys. Res.*, **98,** 7081–7101.

Etcheto, J., and L. Merlivat, 1988: Satellite determination of the carbon dioxide exchange coefficient at the ocean–atmosphere interface: A first step. *J. Geophys. Res.*, **93,** 15 669–15 678.

——, and L. Banege, 1992: Wide-scale validation of Geosat altimeter-derived wind speed. *J. Geophys. Res.*, **97,** 11 393–11 409.

Francis, E., 1987: Calibration of the Nimbus-7 Scanning Multichannel Microwave Radiometer (SMMR), 1979–1984. M.S. thesis, Oregon State University, 248 pp.

Freilich, M. H., and R. S. Dunbar, 1993: Derivation of satellite wind model functions using operational surface wind analyses: An altimeter example. *J. Geophys. Res.*, **98,** 14 633–14 649.

Glazman, R. E., 1991: Statistical problems of wind-generated gravity waves arising in microwave remote sensing of surface winds. *IEEE Trans. Geosci. Remote Sens.*, **29,** 135–142.

Goodberlet, M. A., C. T. Swift, and J. C. Wilkerson, 1989: Remote sensing of ocean surface winds with the Special Sensor Microwave/Imager, *J. Geophys. Res.*, **94,** 14 547–14 555.

Halpern, D., 1993: Validation of Special Sensor Microwave Imager monthly-mean wind speed from July 1987 to December 1989. *IEEE Trans. Geosci. Remote Sens.*, **31,** 692–699.

——, A. Hollingsworth, and F. Wentz, 1994: ECMWF and SSM/I global surface wind speeds. *J. Atmos. Oceanic Technol.*, **11,** 779–788.

Hayes, S. P., L. J. Mangum, J. Picaut, A. Sumi, and K. Takeuchi, 1991: TOGA-TAO: A moored array for real time measurements in the tropical Pacific Ocean. *Bull. Amer. Meteor. Soc.*, **72,** 339–347.

Hollinger, J., 1989: DMSP Special Sensor Microwave/Imager calibration/validation. Final report, Vol 1, Nav. Res. Lab., Washington, D.C.

Kent, E. C., P. K. Taylor, B. S. Truscott, and J. S. Hopkins, 1993: The accuracy of voluntary observing ships meteorological observations—Results of the VSOP-NA. *J. Atmos. Oceanic Technol.*, **10,** 591–608.

Lefevre, J. M., J. Barckicke, and Y. Menard, 1994: A SWH-dependant function for Topex/Poseidon wind speed retrieval. *J. Geophys. Res.*, **99,** 25 035–25 049.

Liu, W. T., 1988: Moisture and latent heat flux variabilities in the tropical Pacific derived from satellite data. *J. Geophys. Res.*, **93,** 6749–6760.

Mangum, L. J., S. P. Hayes, and L. D. Stratton, 1992: Sampling requirements for the surface wind field over the tropical Pacific ocean. *J. Atmos. Oceanic Technol.*, **9,** 668–679.

——, H. P. Freitag, and M. J. McPhaden, 1994: TOGA-TAO array sampling schemes and sensor evaluations. *Oceans '94 OSATES Proc.* Parc de Penfield, Brest, France, **2,** 402–406.

McPhaden, M. J., 1993: TOGA-TAO and the 1991–93 El Niño–Southern oscillation event. *Oceanography,* **6,** 36–44.

Minster, J. F., D. Jourdan, E. Normant, C. Brossier, and M. C. Gennero, 1992: An improved Special Sensor Microwave Imager water vapor correction for Geosat altimeter data. *J. Geophys. Res.*, **97,** 17 859–17 872.

Mo, X. C., and X. Wang, 1994: The global climate of June–August 1992: Warm ENSO episode decays and colder than normal conditions dominate the Northern Hemisphere, *J. Climate,* **7,** 335–357.

Monaldo, F., 1988: Expected differences between buoy and radar altimeter estimates of wind speed and significant wave height and their implications on buoy-altimeter comparisons. *J. Geophys. Res.*, **93,** 2285–2302.

Offiler, D., 1994: The calibration of *ERS-1* satellite scatterometer winds. *J. Atmos. Oceanic Technol.*, **11,** 1002–1017.

Ozieblo, A., and J. Etcheto, 1991: A method for masking microwave radiometer data polluted by the presence of land and ice. *Int. J. Remote Sens.*, **12,** 2379–2388.

Pierson, W. J., Jr., 1990: Examples of, reasons for, and consequences of the poor quality of wind data from ships for the marine boundary layer: Implications for remote sensing. *J. Geophys. Res.*, **95,** 13 313–13 340.

Quilfen, Y., 1993: ERS-1 scatterometer off-line products: Calibration/validation results and case studies. *IGARSS Proceedings,* Tokyo, Japan, 1750–1752.

——, and A. Bentamy, 1994: Calibration/validation of ERS-1 scatterometer precision products, *IGARSS Proceedings.* Pasadena, CA, 945–947.

Waliser, D. E., and C. Gautier, 1993: Comparison of buoy and SSM/I-derived wind speeds in the tropical Pacific. TOGA Notes. 1–7.

Wentz, F. J., 1989: User's manual SSM/I geophysical tapes. Tech. Rep. 060989, Remote Sensing Systems, 16 pp.

——, 1991: User's manual SSM/I antenna temperature tapes, Revision 1. Tech. Rep. 120191, Remote Sensing Systems, 70 pp.

——, 1992: Measurement of oceanic wind vector using satellite microwave radiometers. *IEEE Trans. Geosci. Remote Sens.*, **30,** 960–972.

——, 1993: Revision-2 update for SSM/I geophysical tapes user's manual. Tech. Rep. 040293, Remote Sensing Systems, 8 pp.

Wilkerson, J. C., and M. D. Earle, 1990: A study of differences between environmental reports by ships in the Voluntary Observing Program and measurements from NOAA buoys. *J. Geophys. Res.*, **95,** 3373–3385.

Witter, D. L., and D. B. Chelton, 1991: A Geosat altimeter wind speed algorithm and a method for altimeter wind speed algorithm development. *J. Geophys. Res.*, **96,** 8853–8860.

Young, I. R., 1993: An estimate of the Geosat altimeter wind speed algorithm at high wind speeds. *J. Geophys. Res.*, **98,** 20 275–20 285.